

Electronic Supplementary Information for

Iron-Decorated Nitrogen-Rich Carbons as Efficient Oxygen Reduction Electrocatalysts for Zn-Air Battery

Zhuang Liu,^{a,†} Jing Liu,^{a,†} Hao Bin Wu,^{b,*} Gurong Shen,^a Zaiyuan Le,^a Gen Chen,^a Yunfeng Lu^{a,*}

^aDepartment of Chemical and Biomolecular Engineering, University of California, Los Angeles, CA 90095, USA. Email: luucla@ucla.edu

^bSchool of Materials Science and Engineering, Zhejiang University, Hangzhou 310027, China. Email: hbwu@zju.edu.cn

[†]These authors contribute equally to this work.

Experimental Section

Synthesis of ZIF-8 nanocrystals: ZIF-8 nanocrystals are synthesized by using a simple and scalable co-precipitation method at ambient temperature. In a typical synthesis, 1.47 g of Zn(NO₃)₂·6H₂O was dissolved in 100 mL of methanol. Another solution was prepared by dissolving 1.62 g of 2-methylimidazole in 100 mL of methanol. The later solution was poured into the former one under magnetic stirring, and the stirring was stopped after the two solutions were well mixed. After remaining static for one day at ambient temperature, the white precipitates were collected by centrifugation, washed with methanol and then dried at 80 °C in a vacuum oven over night.

Synthesis of ZIF-8/Fe: To load iron into ZIF-8 nanocrystals, 500 mg of as-prepared ZIF-8 powder was dispersed in 4 mL of iron carbonyl (Fe(CO)₅) under magnetic stirring in a seal glass vial at ambient temperature. After stirring for 4 h, the solid product was collected by filtration and rinsed with ethanol to remove the excess iron carbonyl. The product was finally rinsed with acetone and dried at ambient temperature. Controlled experiments were also performed by extending the stirring time to 8 and 12 h.

Synthesis of Fe-NC catalysts: The as-prepared ZIF-8/Fe was annealed in a tube furnace under N₂ at 800, 900, and 1000 °C for 4 h with a heating rate of 10 °C min⁻¹. The resulting powder was milled using a SPEX 5100 mix mill for 20 min to break down the aggregated particles. NC-900 sample was directly prepared from ZIF-8 nanocrystals at 900 °C without Fe source for comparison.

Synthesis of other M-NC catalysts: To synthesize M-NC catalysts containing other transition metals, 100 mg of corresponding solid metal carbonyls (Mn₂(CO)₁₀, Co₂(CO)₈, Mo(CO)₆, W(CO)₆) are dissolved in an appropriate amount of diethyl ether. And then 200 mg of ZIF-8 nanocrystals was added into the above solution. After stirring at ambient temperature for 16 h, the product was collected by filtration and rinsed by diethyl ether. The as-obtained precursor was subjected to the same heat treatment at 900 °C for 4 h in nitrogen.

Materials Characterizations: Powder X-ray diffraction was operated on a Rigaku MiniFlex II (Rigaku, Japan) using Cu K α radiation ($\lambda=0.15406$ nm). Nitrogen-sorption isotherms were measured at 77 K with a Micromeritics ASAP 2020 analyzer (Micromeritics Instrument Corporation, Norcross, GA). Specific surface areas were calculated by the Brunauer-Emmett-Teller (BET) method and the micropore surface areas were obtained by the t-plot method. Morphology and structure of the samples were characterized by scanning electron microscope (SEM, FEI Nova NanoSEM) and transmission electron microscope (TEM, FEI T12, 120 kV). Elemental composition was analyzed by energy-dispersive X-ray spectroscopy (EDS) attached on SEM. Thermogravimetric analysis (TGA) and differential scanning calorimetry (DSC) was conducted on a TA Instruments SDT-Q600 under N₂ flow with a heating rate of 10 °C min⁻¹.

Electrochemical measurements: All electrocatalytic measurements are carried out in a three-electrode cell using a rotating disk electrode (RDE, PINE Research Instrumentation) with a Bio Logic VMP3 (Bio Logic Science Instruments) and a WaveDriver 20 (PINE Research Instrumentation) electrochemical workstations at ambient temperature. A graphite rod and a

Ag/AgCl (saturated KCl) were used as the counter and reference electrodes, respectively. A glassy carbon (GC) electrode was used as the substrate for the working electrode. To prepare the working electrode, 5 mg of the catalyst was dispersed in 2 mL of ethanol and 30 μ L of 5wt% Nafion solution by ultrasonication. A certain volume of the suspension was pipetted on the GC surface and dried at ambient temperature. RDE measurements for ORR were performed in O_2 saturated 0.1 M NaOH as electrolyte with a scan rate of 10 mV s⁻¹. The polarization curves were recorded using positive scan, and corrected with background current and iR loss. Background current was scanned in N_2 saturated 0.1 M NaOH. Solution resistance determined by the high frequency intercept in the Nyquist plot from electrochemical impedance spectrum and used for iR correction. Onset potential is defined as the potential to reach a current density of 0.1 mA cm⁻². Potentials in this study refer to reversible hydrogen electrode (RHE). The reference electrode was calibrated by conducting cyclic voltammetry (CV) scan with Pt/C on GC as working electrode in H_2 saturated 0.1 M NaOH. The potential where current crossed zero was the thermodynamic potential for the hydrogen electrode reaction. In 0.1 M NaOH, $E(RHE) = E(Ag/AgCl) + 0.942$ V. Stability of the catalysts were evaluated by conducting CV scans between 0.6-1 V vs. RHE at 100 mV s⁻¹ in O_2 saturated electrolyte for 5000 cycles.

Zinc-Air Battery Assembly: Fe-NC-900-M was dispersed in ethanol to form an ink, which was hot sprayed onto carbon paper to form the air cathode. The mass loading was 0.73 mg cm⁻². Polished Zn foil and 6 M KOH were used as anode and electrolyte respectively. Zinc-air battery with 40 wt% Pt/C as cathode catalyst was assembled following the same method and total catalyst loading for comparison. Zinc-air battery test was performed on a WaveDriver 20 (PINE Research Instrumentation) electrochemical workstations at ambient temperature.

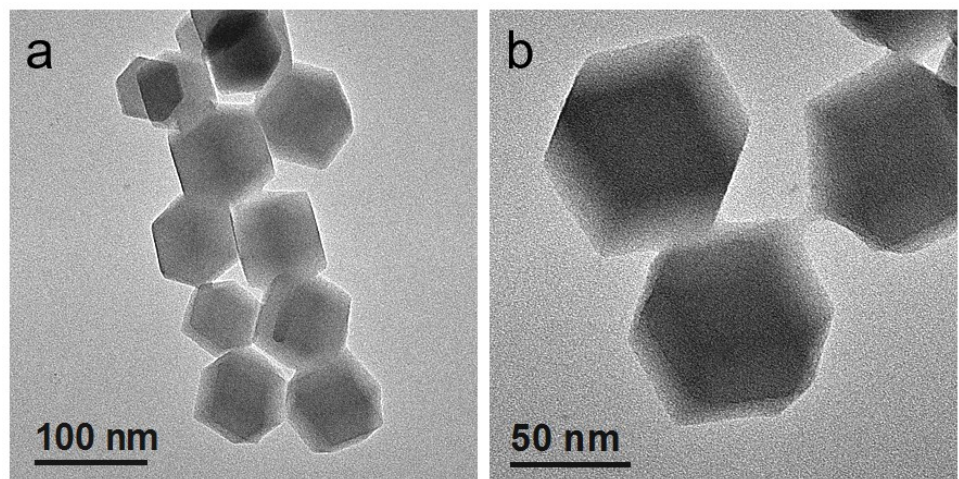


Fig. S1. TEM images of ZIF-8 nanocrystals.

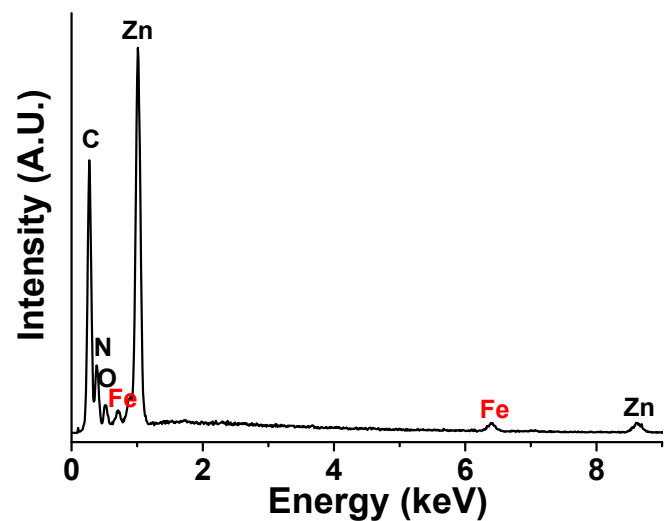


Fig. S2. EDS spectrum of the ZIF-8/Fe.

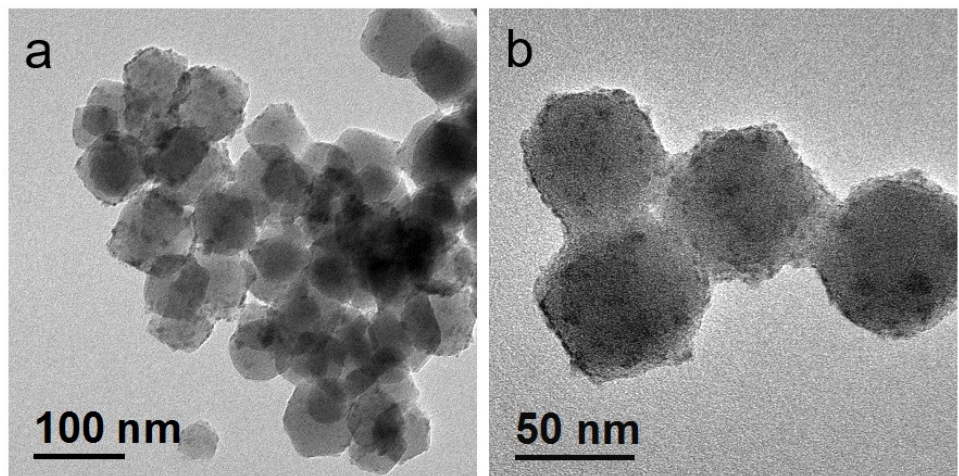


Fig. S3. TEM images of ZIF-8/Fe.

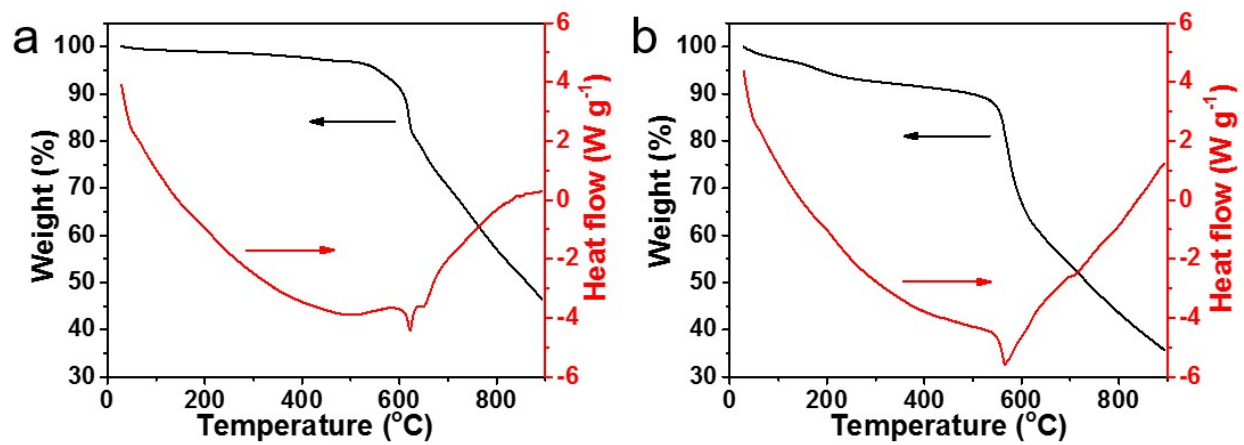


Fig. S4. TGA and DSC curves of (a) ZIF-8 and (b) ZIF-8/Fe in N_2 flow.

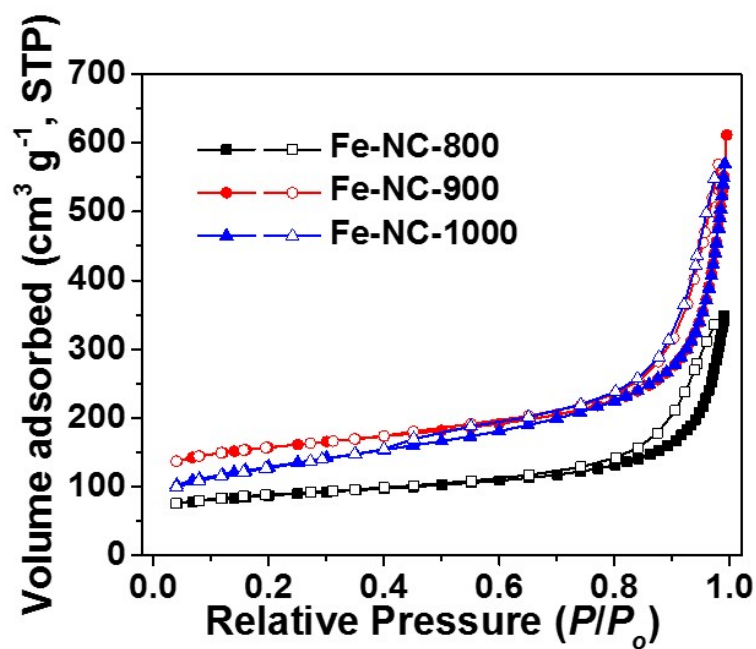


Fig. S5. N_2 adsorption-desorption isotherms of Fe-NC catalysts.

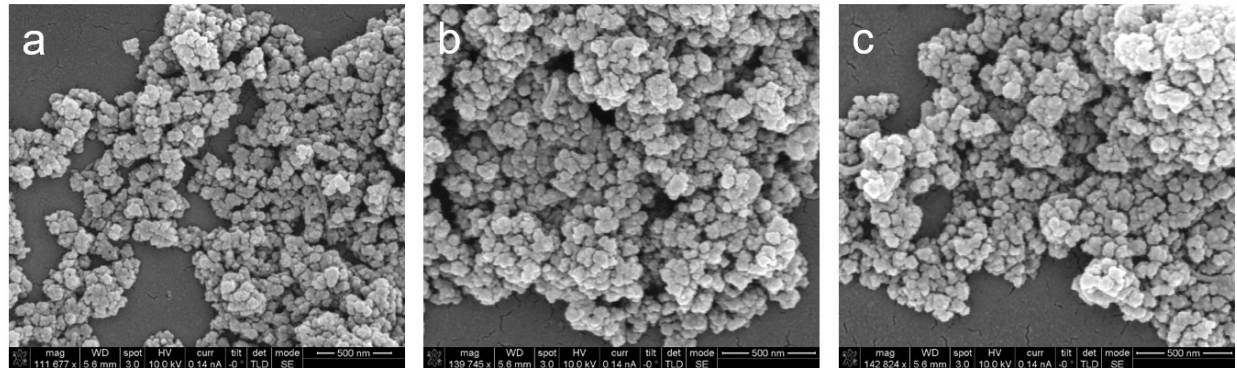


Fig. S6. SEM images of (a) FE-NC-800, (b) Fe-NC-900 and (c) Fe-NC-1000. Scale bars are 500 nm.

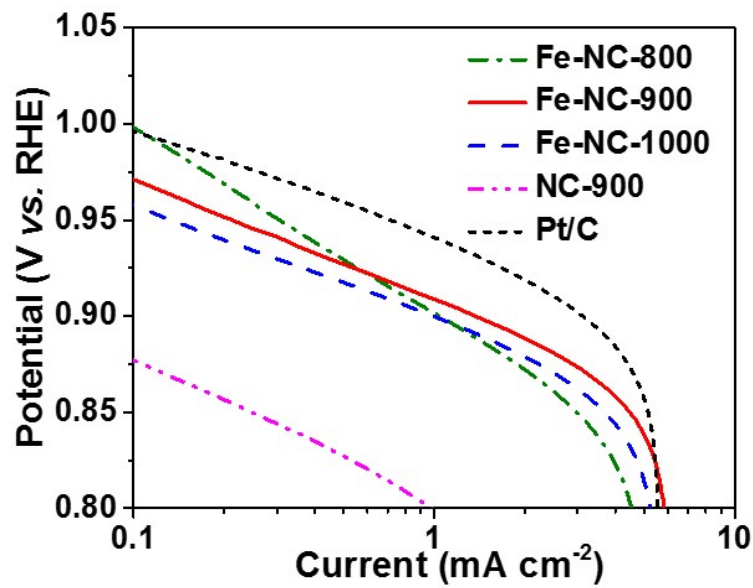


Fig. S7. Tafel plots of Fe-NC catalyst, NC-900 and Pt/C derived from the polarization curves shown in Figure 3c.

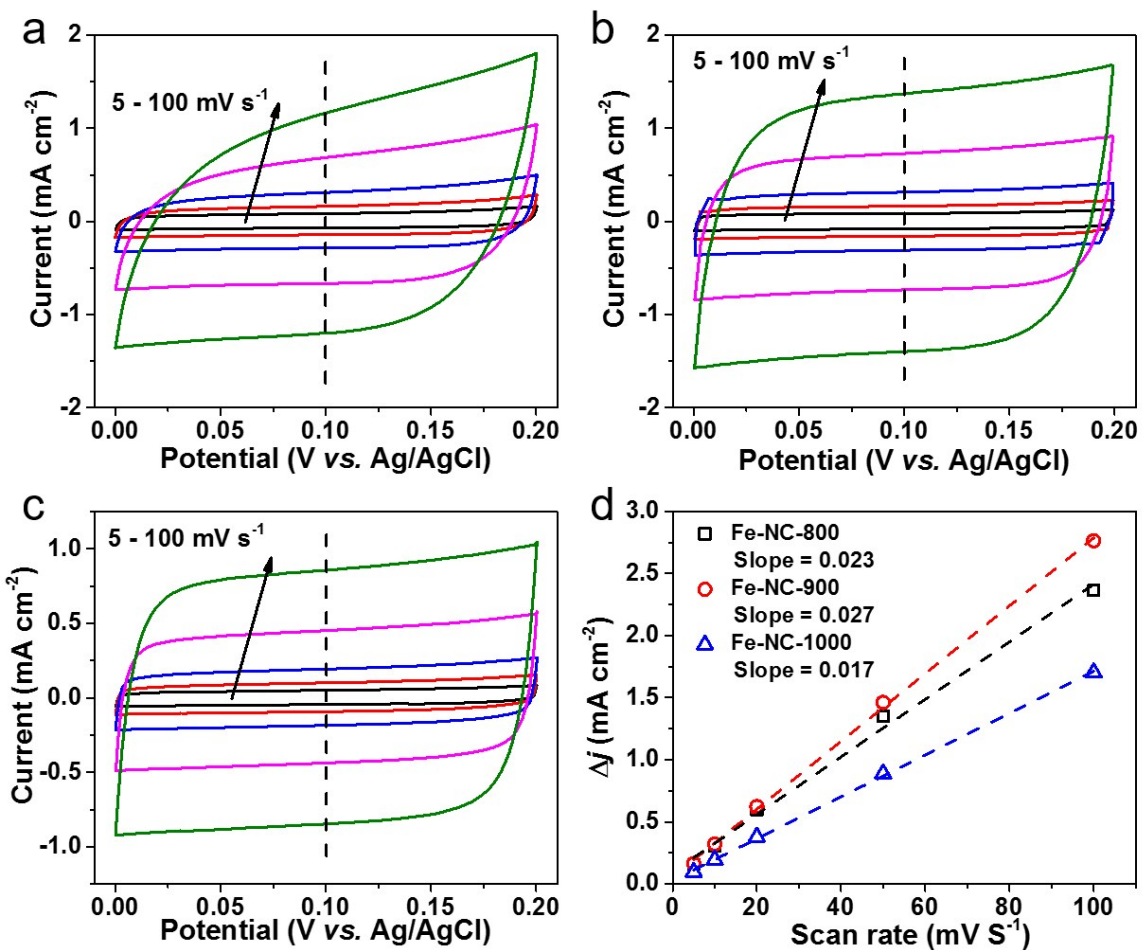


Fig. S8. CV profiles of (a) Fe-NC-800, (b) Fe-NC-900, and (c) Fe-NC-1000 at scan rates of 5, 10, 20, 50, 100 mV s⁻¹ in N₂ saturated 0.1 M NaOH. (d) Current density differences (Δj) plotted against scan rates. Δj is the difference between anodic and cathodic current densities at potential indicated by the black dash lines, where no redox current peaks are observed. The linear slopes in (d) are equivalent to twice of the electrochemical double-layer capacitances (C_{dl}). C_{dl} is generally used to represent the electrochemical surface area (ECSA).

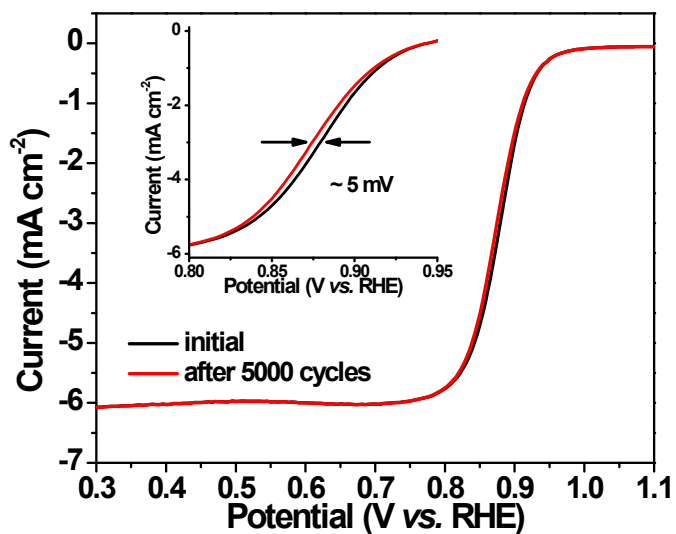


Figure S9. Polarization curves of Fe-NC-900 before and after 5000 CV cycles (inset shows the enlarged polarization curve) in 0.1 M NaOH at 1600 rpm.

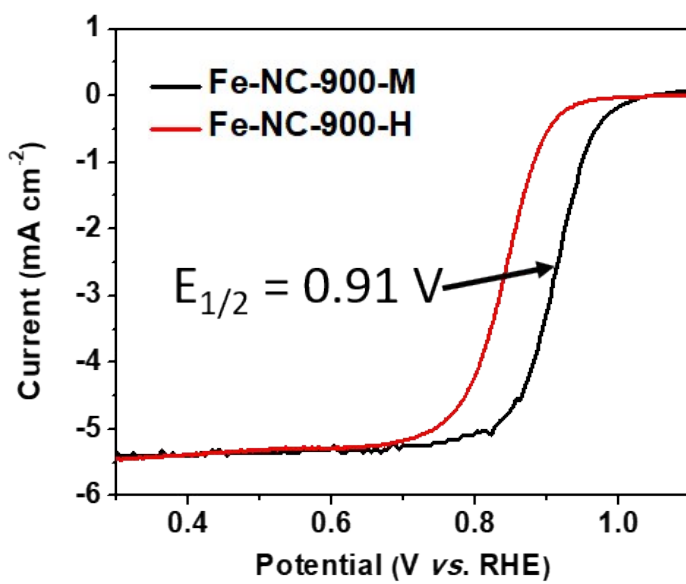


Figure S10. ORR polarization curves of Fe-NC-900-M and Fe-NC-900-H in 0.1 M NaOH at 1600 rpm.

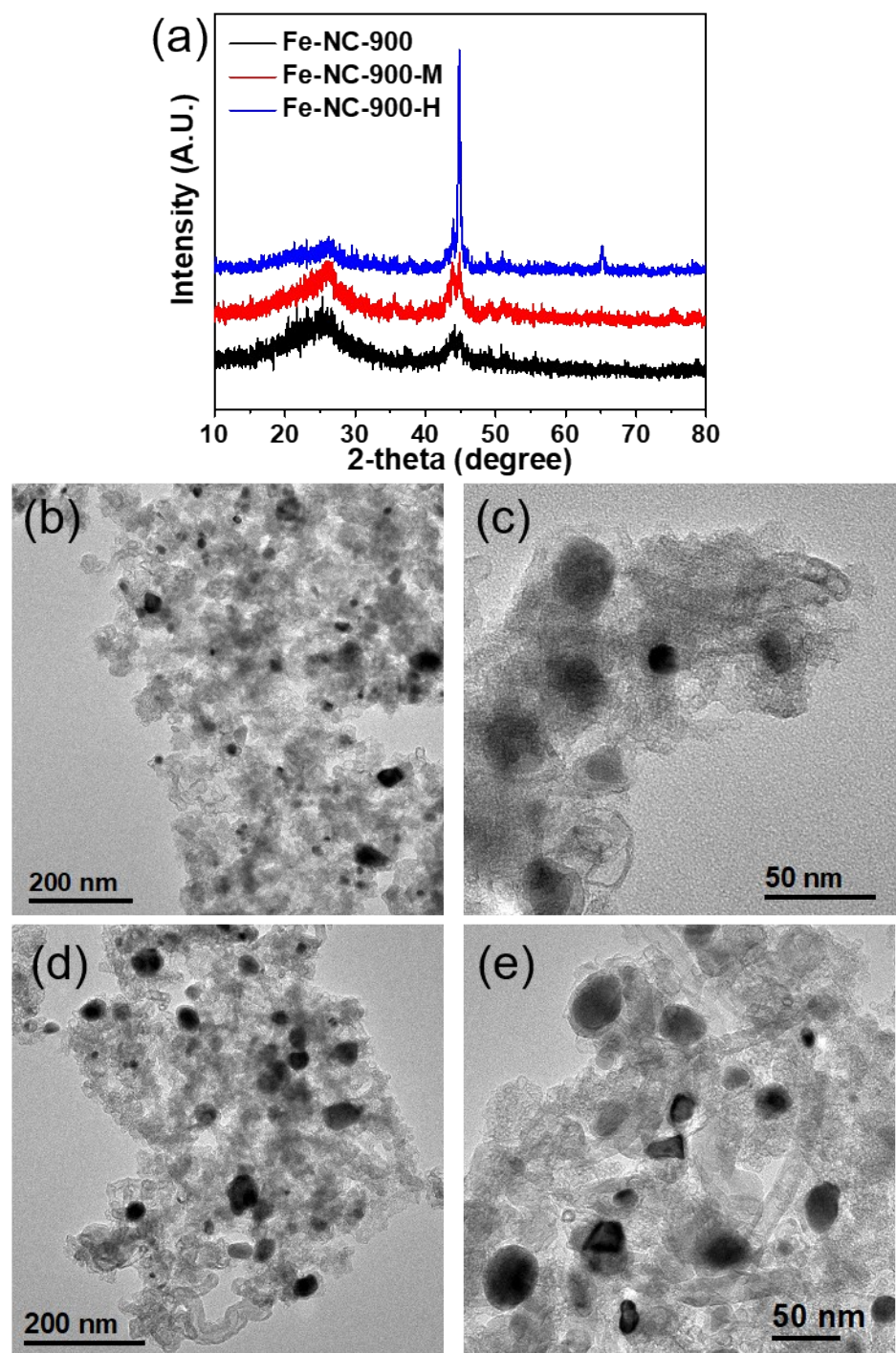


Figure S11. (a) XRD patterns of Fe-NC-900 catalysts with different Fe loading. TEM images of (b, c) Fe-NC-900-M and (d, e) Fe-NC-900-H.

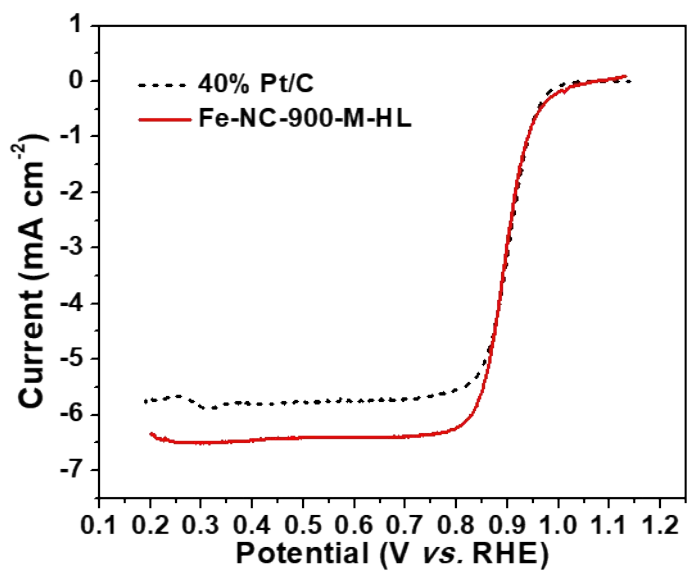


Figure S12. ORR polarization curves of Fe-NC-900-M-HL and Pt/C catalyst in 0.1 M NaOH at 1600 rpm.

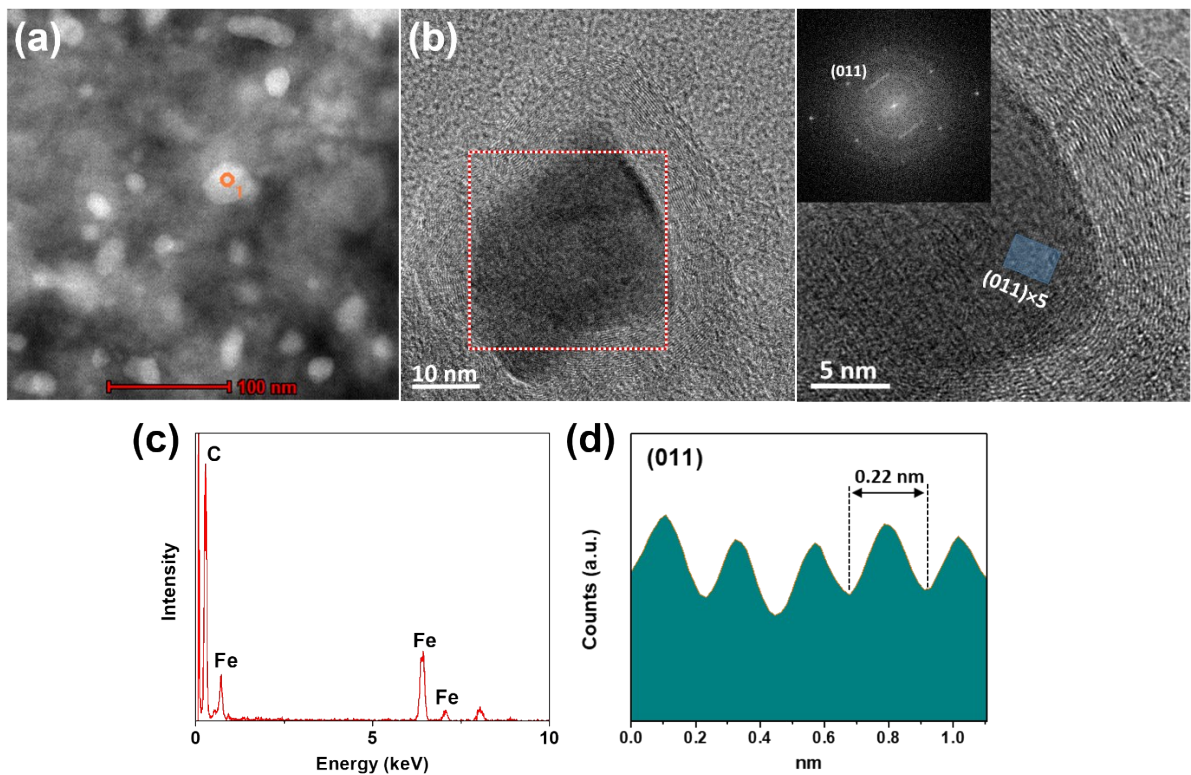


Figure S13. (a, b) HAADF-STEM image and HRTEM image of Fe-NC-900-M (the inset in b being the fast Fourier transform of the TEM image of a typical nanoparticle). (c) EDS point-shot spectrum of the spot denoted in (a). (d) Contrast profile of the area shown in (b).

As shown in Figure S13a, Fe-NC-900-M contains uniformly distributed nanoparticles of under 40 nm in diameter. The EDS spectrum of one typical nanoparticle reveals its composition to be primarily iron and carbon (Figure S13c). The HRTEM image and the corresponding fast-Fourier-transform of a typical nanoparticle further reveals its crystalline structure (Figure S13b and d). The continuous lattice distance of 0.22 nm should be attributed to the (011) planes of metallic iron (cubic) or (220) planes of Fe_3C , which agrees well with the EDS and XRD results.

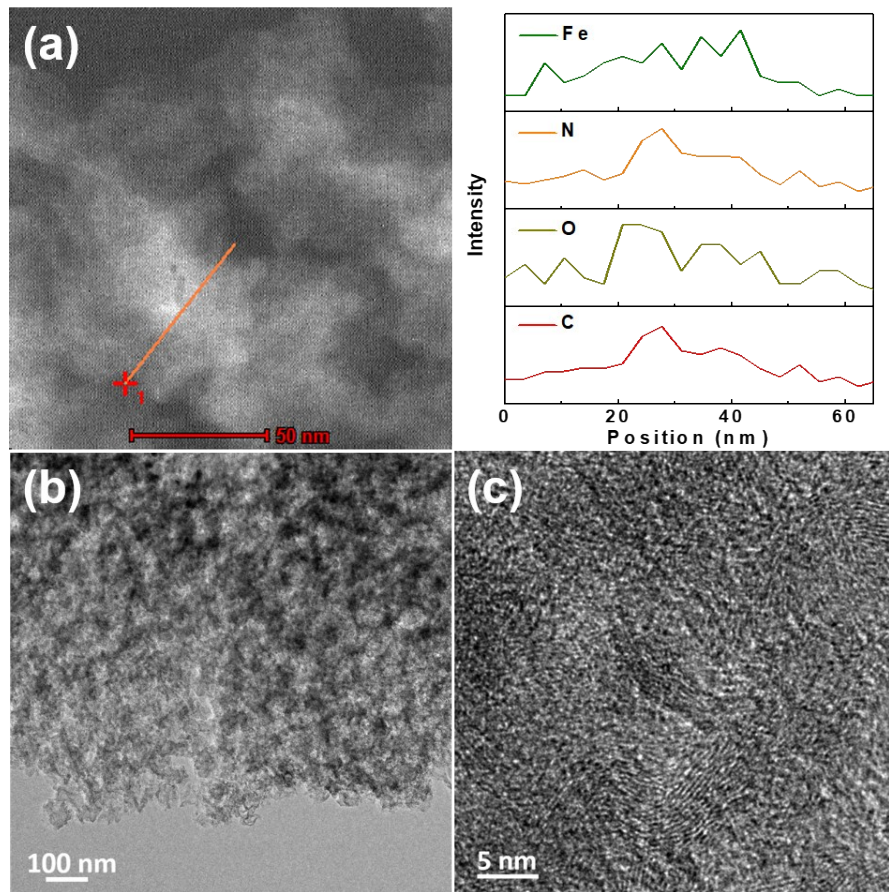


Figure S14. (a) HAADF-STEM image of Fe-NC-900-M-AW and the EDS linear scan spectrum corresponding to the line in the image, (b, c) TEM image of Fe-NC-900-M-AW.

As shown in Figure S14a, the HAADF-STEM image of Fe-NC-900-M-AW reveals that Fe/Fe₃C nanoparticles in Fe-NC-900-M are thoroughly removed after acid washing. However the remaining uniformly distributed angstrom level bright dots on the carbon scaffold should correspond to the iron atom reserved in Fe-N_x moieties. The EDS linear scan reveals the existence of C, N, O and Fe in the sample, and their even distribution across the line, proving the uniform distribution of these elements in the catalyst. Normal TEM image of Fe-NC-900-M-AW (Figure S14b) confirms the absence of nanoparticle in the sample, and the HRTEM image in Figure S14c shows an empty graphitic shell where the Fe-based nanoparticle has been removed by acid washing. The preservation of Fe-N_x in Fe-NC-900-M-AW is further proved by its XPS Fe 2p spectrum (Figure S15), which shows the pronounced peak at around 710 eV, similar to that of Fe-NC-900 in Figure 3.

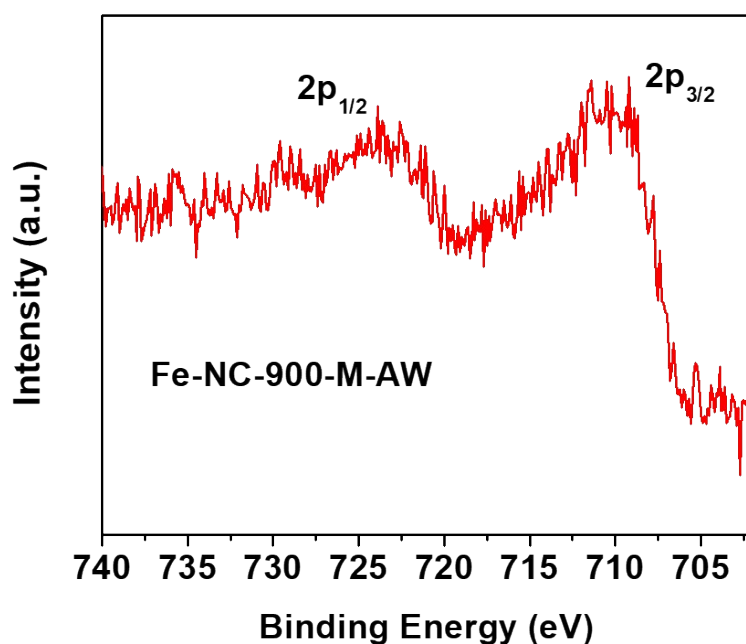


Figure S15. XPS Fe 2p spectrum of Fe-NC-900-M-AW.

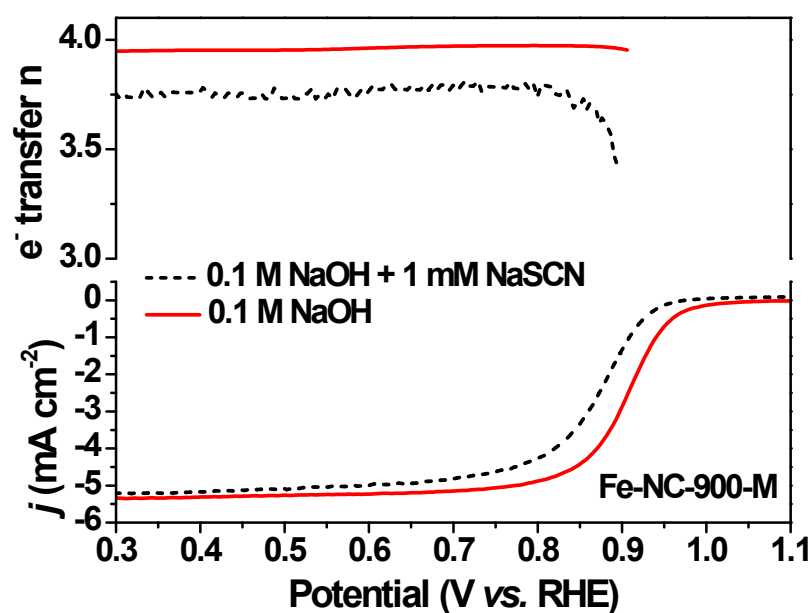


Figure S16. Polarization curves and the corresponding electron transfer number of Fe-NC-900-M (loading: 0.25 mg cm^{-2}) in 0.1 M NaOH with and without 1 mM NaSCN at 1600 rpm .

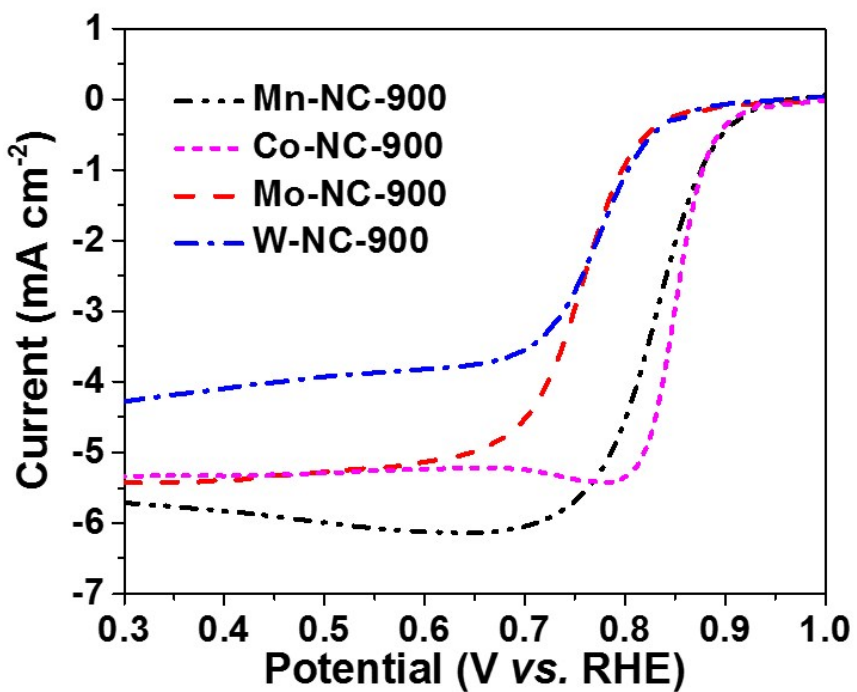


Figure S17. Polarization curves of M-NC catalysts with different transition metals in 0.1 M NaOH at 1600 rpm (loading: 0.5 mg cm^{-2}).

Table S1. Comparison of various noble-metal free electrocatalysts for ORR in alkaline electrolyte.

Catalysts	Loading (mg cm ⁻²)	Electrolyte	Onset Potential (V vs. RHE)	Half-wave Potential (V vs. RHE)	Reference
Fe-NC-900	0.25	0.1 M NaOH	0.97	0.88	This work
Fe-NC-900-M	0.25	0.1 M NaOH	1.02	0.91	This work
Co₃O₄/N-rmGO	0.17	0.1 M KOH	0.88	0.83	<i>Nat. Mater.</i> 2011 , <i>10</i> , 780
NPMC-1000	0.15	0.1 M KOH	0.94	0.85	<i>Nat. Nano.</i> 2015 , <i>10</i> , 444
Co@Co₃O₄@C-CM	0.1	0.1 M KOH	0.93	0.81	<i>Energy Environ. Sci.</i> 2015 , <i>8</i> , 568
(Fe, Mn)-N-C-3HT-2AL	0.8	0.1 M KOH	0.98	0.90	<i>Nat. Commun.</i> 2015 , <i>6</i> , 8618
FePhen@MOF-ArNH₃	0.6	0.1 M KOH	1.03	0.86	<i>Nat. Commun.</i> 2015 , <i>6</i> , 7343
N/Co-doped PCP//NRGO	~0.7	0.1 M KOH	0.97	0.86	<i>Adv. Funct. Mater.</i> 2015 , <i>25</i> , 872
[FeCo]O₄/NG	0.6	0.1 M KOH	0.98	0.866	<i>Angew. Chem. Int. Ed.</i> 2016 , <i>55</i> , 1340
CNT/PC	0.8	0.1 M KOH	NA	0.88	<i>J. Am. Chem. Soc.</i> 2016 , <i>138</i> , 15046
Co SAs/N-C(900)	0.408	0.1 M KOH	0.982	0.881	<i>Angew. Chem. Int. Ed.</i> 2016 , <i>55</i> , 10800
Fe@C-FeNC-2	0.7	0.1 M KOH	NA	0.899	<i>J. Am. Chem. Soc.</i> 2016 , <i>138</i> , 3570
{Co}[FeCo]O₄/NG	0.6	0.1 M KOH	0.98	0.866	<i>Angew. Chem. Int. Ed.</i> 2016 , <i>55</i> , 1340
N,P-HPC	0.8	0.1 M NaOH	0.924	0.853	<i>J. Mater. Chem. A.</i> , 2017 , <i>5</i> , 24329
Fe-ISAs/CN	0.408	0.1 M KOH	0.986	0.90	<i>Angew. Chem. Int. Ed.</i> 2017 , <i>56</i> , 6937
S,N-Fe/N/C-CNT	0.6	0.1 M KOH	NA	0.85	<i>Angew. Chem. Int. Ed.</i> 2017 , <i>56</i> , 610
1000-CNS	0.14	0.1 M KOH	0.99	0.85	<i>Energy Environ. Sci.</i> 2017 , <i>10</i> , 742
CF-NG-Co	0.28	0.1 M NaOH	0.97	0.88	<i>J. Mater. Chem. A.</i> , 2018 , <i>6</i> , 489
FeN_x-PNC	0.14	0.1 M KOH	0.997	0.86	<i>ACS Nano</i> 2018 , <i>12</i> , 1949

Table S2. Comparison of zinc-air battery utilizing Fe-NC-900-M with other noble-metal free electrocatalysts reported recently.

Catalysts	Loading (mg cm ⁻²)	Open circuit Voltage (V)	Peak power (mW cm ⁻²)	Reference
Fe-NC-900-M	0.73	1.5	271	This work
Co-N-CNT	1	1.365	101	<i>Adv. Funct. Mater.</i> 2018 , 28, 1705048
CF-NG-Co	1	1.49	160	<i>J. Mater. Chem. A</i> 2018 , 6, 489
1100-CNS-4	2	1.49	151	<i>Energy Environ. Sci.</i> 2017 , 10, 742
S,N-Fe/N/C-CNT	1.25	1.35	102.7	<i>Angew. Chem. Int. Ed.</i> 2017 , 56, 610
N-GCNT/FeCo	2	1.48	89.3	<i>Adv. Energy Mater.</i> 2017 , 7, 1602420
N-HCNs	1	1.49	76	<i>Nanoscale.</i> 2017 , 9, 13257
Fe/N/C@BMZIF	1	1.48	235	<i>ACS Appl. Mater. Interfaces</i> 2017 , 9, 5213
PFe-Pc	2	1.6	192	<i>Dalton Trans.</i> 2017 , 46, 1803
Fe,N-CNS	1	~1.375	221	<i>Adv. Sustainable Syst.</i> 2017 , 1, 1700085
Co/Co_xS_y@SNCF-800	2	1.37	230	<i>ACS Appl. Mater. Interfaces</i> 2017 , 9, 34269
Fe₂N@NC	1	1.48	82.3	<i>Catal. Sci. Technol.</i> 2017 , 7, 5670
Co₄N/CNW/CC	1	1.4	174	<i>J. Am. Chem. Soc.</i> 2016 , 138, 10226
Co₃O₄-NCNT/SS	NA	NA	160.7	<i>Adv. Mater.</i> 2016 , 28, 6421
Fe/Fe₂O₃@Fe-N-C	2	1.47	220	<i>Nano Res.</i> 2016 , 9, 2133
Fe@N-C-700	2.2	1.4	220	<i>Nano Energy</i> 2015 , 13, 387
CoO/N-CNT	1	1.4	265	<i>Nat. Commun.</i> 2013 , 4, 1805